Journal of Neuroscience Research 89:729–743 (2011)

Hypothermia Prevents Nitric Oxide System Changes in Retina Induced by Severe Perinatal Asphyxia

**Manuel Rey-Funes,[1] Mariano Esteban Ibarra,[1] Verónica Berta Dorfman,[1] Julia Serrano,[2] Ana Patricia Fernández,[2] Ricardo Martínez-Murillo,[2] Alfredo Martínez,[2,3] Héctor Coirini,[4] José Rodrigo,[2] and César Fabián Loidl[1]*

[1]Laboratorio de Neuropatología Experimental, Instituto de Biología Celular y Neurociencia "Prof. E. De Robertis," Facultad de Medicina, Universidad de Buenos Aires, CONICET, Ciudad Autónoma de Buenos Aires, Argentina
[2]Departamento de Neurobiología Celular, Molecular y del Desarrollo, Instituto Cajal, CSIC, Madrid, España
[3]Grupo de Estudio de Angiogénesis, Centro de Investigación, Biomédica de La Rioja, unidad asociada CIBIR-CSIC, Logroño, España
[4]Laboratorio de Neurobiología, Instituto de Biología y Medicina Experimental, CONICET, Ciudad Autónoma de Buenos Aires, Argentina—Departamento de Bioquímica Humana, Facultad de Medicina, Universidad de Buenos Aires, Ciudad Autónoma de Buenos Aires, Argentina

One-third of asphyctic neonates develop long-term neurological injuries, including several degrees of ischemic proliferative retinopathy (IPR) such as retinopathy of prematurity (ROP). Given that the retina is altered by perinatal asphyxia, our aim was to study the effects of nitric oxide (NO) in the retina in order to analyze its impact on the retinal injury. Application of hypothermia was evaluated as preventive treatment. Sprague-Dawley rats were subjected to perinatal asphyxia [either at 37°C (PA group) or at 15°C (HYP group)]. Full-term rats were used as controls (CTL). A significantly increased activity of both constitutive NO synthase (nNOS, Ca^{2+}-dependent) and inducible NO synthase (iNOS, Ca^{2+}-independent) was observed in PA retinas from 21 days old up to 60 days old with respect to age-matched CTL, with a significant increase along the time course in the PA. nNOS was immunolocalized at amacrine, horizontal, and ganglion cells of the PA group, with a significant increase in relative optical density (R.O.D.), cellular area, and number of cells. iNOS immunoreactivity was observed in the inner nuclear layer and in the internal Müller cell processes of PA, with a significant increase in R.O.D. and colocalizing with GFAP in the 60-day-old PA group. Six nitrated protein species were increased in retinas from PA rats. Nitrotyrosine immunoreactivity showed a localization similar to that of iNOS, with increased R.O.D. in the PA group and colocalization with GFAP in 60-day-old animals. HYP prevented all the changes observed in PA rats. Although the NO system displays changes induced by hypoxia-ischemia, hypothermia application shows a strong protective effect.

Key words: retina; ischemic proliferative retinopathy; retinopathy of prematurity; nitrotyrosine; rat

Perinatal asphyxia is the world's most severe problem in Perinatology Services (Cunningham et al., 2005; WHO, 1991). One-third of asphyctic neonates develop serious long-term neurological injuries, including several degrees of ischemic proliferative retinopathy (IPR) such as retinopathy of prematurity (ROP; Hill, 1991; Younkin, 1992; Palmer and Vannucci, 1993; Rivkin, 1997). ROP is an avoidable cause of visual impairment and blindness. Children exposed to hyperoxia during neonatal intensive care are highly susceptible to developing ROP. Two phases are described in the development of ROP: the first begins with oxidative injury, which damages the vascular endothelium and blocks the formation of new vessels, generating a nonvascular retinal area. The second phase is characterized by increased angiogenesis (Hardy et al., 2000; Jankov et al., 2001; Smith, 2003) and damage as a result of blood reperfusion with toxic oxygen tension in the immature retinal tissue (Smith, 2003). We have recently described how animals exposed to perinatal asphyxia develop retinal morphological injuries compatible with ROP, including ganglion cell degeneration, neovascularization of the inner

Contract grant sponsor: UBA; Contract grant number: M039; Contract grant sponsor: CONICET; Contract grant number: PIP 5349.

*Correspondence to: C.F. Loidl, MD, PhD, "Laboratorio de Neuropatología Experimental," Instituto de Biología Celular y Neurociencia "Prof. Eduardo De Robertis," Facultad de Medicina, Universidad de Buenos Aires, CONICET, Paraguay 2155 3° Piso, Ciudad Autónoma de Buenos Aires, Argentina. E-mail: cfloidl@yahoo.com.ar

Received 30 March 2010; Revised 19 October 2010; Accepted 20 October 2010

Published online 17 February 2011 in Wiley Online Library (wileyonlinelibrary.com). DOI: 10.1002/jnr.22556

retina (IR; including the inner limiting layer, the optic nerve fiber layer, and the ganglion cell layer), and Müller cell hypertrophy in the innermost layers of the retina (inner nuclear layer, inner plexiform layer, and IR; Rey-Funes et al., 2010).

Global perinatal asphyxia originates a hypoxia-ischemia status, which damages the brain, spinal cord, and retina (Loidl et al., 1994, 1998, 2000; Dorfman et al., 2009; Rey-Funes et al., 2010). The seriousness of the degree and the length of the perinatal asphyxia with lack of oxygen are decisive for the development of injury sequelae such as attention-deficit hyperactivity disorder (ADHD; American Psychiatric Association, 1987), epilepsy, mental retardation, spasticity, and visual and hearing alterations (Crofts et al., 1998; Younkin, 1992).

NO is one of the most widespread intercellular messengers in the retina (Eldred and Blute, 2005). In the newborn retina, NO is involved in neuroprotective processes (Hardy et al., 2000; Osborne et al, 2004). NO synthase (NOS) is the enzyme responsible for catalyzing the oxidation of L-arginine, yielding equimolar amounts of NO and L-citrulline (Moncada et al., 1997). There are two constitutive Ca^{2+} dependent isoforms of NOS, endothelial (eNOS) and neuronal (nNOS), and one inducible isoform (iNOS) that is Ca^{2+} independent. nNOS and iNOS expression and activity have been described in the brain, spinal cord, and retina of mammals (Venturini et al., 1991; Zhang et al., 1993; Saito et al., 1994; Uttenthal et al., 1998; Pullen and Humphreys, 1999; Rodrigo et al., 2001; Dorfman et al., 2004). NOS immunolocalization in the retina has been confirmed in amacrine and ganglion cells, Müller cells, photoreceptors, and nerve fibers in the inner and outer plexiform layers of the retina (Dawson et al., 1991; Yamamoto et al., 1993; Goureau et al., 1994; Kobayashi et al., 2000).

Oxygen deprivation induces overproduction of NO (Beckman, 1990; Bredt and Snyder, 1992), and its excess is toxic to cells (Moncada and Higgs, 1991; Moncada et al., 1991). NO reacts with the free radical superoxide, exacerbating neurodegenerative processes through the formation of peroxynitrites, which promote protein nitration (Beckman, 1990, 1996; Koppal et al., 1999; Alonso et al., 2002; Castro-Blanco et al, 2003). High levels of NO produced at perinatal asphyxia induce alterations in NOS expression, activity, and protein nitration (Loidl et al., 1998; Dorfman et al., 2009). NO is postulated as a key neurotoxic factor of ROP (Osborne et al., 2004), and an increase in NO concentration in retina induces cytotoxic effects (Chemtob et al., 1995; Hardy et al., 1996).

Animal studies have shown that a reduction in core temperature protects cells against damage by a reduction of reactive oxygen species and an inhibition of the toxic release of NO (Lei et al., 1997; Loidl et al., 1998; Ekimova, 2003; Gisselsson et al., 2005; Dorfman et al., 2009). The use of hypothermia has been proposed as a treatment to reduce secondary neuronal injury after severe perinatal hypoxia ischemia in humans (Gunn, 2000; Katz et al., 2004; Gisselsson et al., 2005). Selective head cooling (10°C) plus mild systemic hypothermia (34.5–35°C) has been applied to term infants with hypoxic-ischemic encephalopathy in clinical research protocols (Battin et al., 2003).

Given that the inner layers of the retina are particularly sensitive to oxygen shortage (Osborne et al., 2004), and in accordance with recently published results showing morphological retinal alterations induced by perinatal asphyxia (Rey-Funes et al., 2010), the aim of the present work was to study the effect of perinatal asphyxia on NOS activity and expression in the retina in order to analyze and evaluate the impact of NO on the retinal injury. The application of hypothermia was evaluated as a neuroprotective treatment.

MATERIALS AND METHODS

Hypoxic-Ischemic Injury

Severe perinatal asphyxia was induced by using a noninvasive model of hypoxia-ischemia as described previously (Loidl et al., 2000). Sprague-Dawley albino rats with genetic quality and sanitary certification from the animal facility of our institution, were cared for in accordance with the guidelines published in the NIH *Guide for the care and use of laboratory animals* (National Institutes of Health Publication No. 85-23, revised 1985), and the principles presented in the "guidelines for the use of animals in neuroscience research" by the Society for Neuroscience (published in Membership Directory of the Society, 1992). The animal model described below has been approved by the Ethical Committee of CICUAL: "Comité Institucional para el Uso y Cuidado de Animales de Laboratorio" (Resolution No. 2079/07), Facultad de Medicina, Universidad de Buenos Aires. Appropriate proceedings were performed to minimize the number of animals used and their suffering, pain, and discomfort. Animals were kept under standard laboratory conditions at 24°C, with light/dark cycles of 12/12 hr, and food and water were given ad libitum. Thirty-two timed-pregnant Sprague-Dawley rats were sacrificed by decapitation and immediately hysterectomized after their first pup had been delivered vaginally (CTL, n = 5). Full-term fetuses, still inside the uterus, were subjected to asphyxia performed by transient immersion of both uterine horns in a water bath at 37°C for 20 min (PA, n = 5 per group) or at 15°C for 20 min (HYP, n = 5). Hypothermia was selected at 15°C as it previously showed to allow the highest survival rate (Loidl et al, 1993; Loidl, 1997). After asphyxia, the uterine horns were opened, pups were removed, dried of delivery fluids, and stimulated to breathe, and their umbilical cords were ligated. The pups were then placed for recovery under a heating lamp and given to a surrogate mother. Time of asphyxia was measured as the time elapsed from the hysterectomy up to the recovery from the water bath. The overall mortality rate was similar to that previously reported (Loidl et al., 2000), 60% for the PA group at 37°C and 0% for the HYP group. To avoid the influence of hormonal variations resulting from the female estrous cycle, only male rats were included in this study.

NOS Activity

PA, HYP, and CTL animals 7, 15, 21, 30 and 60 days of age (PND7, PND15, PND21, PND30, and PND60, respectively) were deeply anaesthetized by intraperitoneal

injection of cloral hydrate 28% P/V (0.1 ml/100 g body weight), sacrificed by decapitation, and enucleated. Anterior segments of the eyes, including the lense, were discarded and the retinas dissected from the posterior segment, frozen, and stored at –80°C until use. The activities of nNOS and iNOS were determined by measuring the conversion of L-(U-^{14}C)arginine into L-(U-^{14}C)citruline as in the assay described by Radomski et al. (1993). Briefly, tissues were homogenized (1:3 w/v) at 4°C in HOSF buffer [20 mM HEPES, 0.2 M sucrose, 5 mM DTT, 1 mM ethylenediaminetetraacetic acid (EDTA), 10 μg/ml soybean trypsin, 10 μg/ml leupeptin, 2 μg/ml pepstatin, 0.1 mM PMSF, pH 7.4]. Homogenates were ultrasonicated and centrifuged for 30 min at 15,000 rpm (4°C) and supernatants collected. To use similar amounts of proteins from each sample, protein concentration was determined by the Bradford method (Bradford, 1976), using bovine serum albumin as standard. Then, samples of supernatants were incubated for 20 min, at 37°C with 20 μM L-(U-^{14}C)arginine in incubation buffer (50 mM KH_2PO_4, 0.2 mM $CaCl_2$, 50 mM L-valine, 1 mM L-citruline, 1.5 mM DTT and 1 mM de $MgCl_2$, pH 7.4 with KOH 2 N, plus 0.75 μg/ml NADPH, 2.15 μg/ml FMN, 3.74 μg/ml FAD and 1.412 μg/ml BH_4). The reaction was stopped with addition of Dowex-50 WX8-400 ionic interchange resin, and the resultant supernatant containing L-(U-^{14}C)citruline was quantified. To determine the activity of nNOS, we calculated the difference between the amount of (^{14}C)citruline produced in control samples and that in the samples processed in incubation buffer containing 2 mM ethylene glycol bis(β-aminoethyl ester)-N-N^1-tetraacetic acid (EGTA). To obtain the activity of iNOS, we calculated the difference between the amount of [^{14}C]citruline produced in samples containing 2 mM EGTA and that in the samples processed with incubation buffer containing 2 mM EGTA and 2 mM L-NAME.

Immunohistochemistry

PA, HYP, and CTL rats 21 and 60 days of age (PND21 and PND60, respectively) were deeply intraperitoneally anaesthetized with cloral hydrate 28% P/V (0.1 ml/100 g body weight) and intracardially perfused with physiological solution followed by 4% paraformaldehyde in 0.1 M, pH 7.4, phosphate buffer at 4°C. After enucleating, anterior segments of the eyes, including the lense, were taken off and discarded, and the posterior segments of the eyes containing the retinas were postfixed overnight. After cryoprotection with an increasing series of sucrose (10%, 20%, and 30%) in phosphate-buffered saline 0–4°C overnight, tissues were included in Tissue Tec, frozen in powdered dry ice, and stored at –80°C. Sections (15 μm thick) were obtained using a Leitz ''Lauda'' cryostat and mounted onto gelatin-coated slides (2.5% gelatin, 1% Elmer's glue), air dried at room temperature, and stored at –80°C until use. For the immunohistochemical assay, endogenous peroxidase activity was blocked with 1% hydrogen peroxide in phosphate buffer for 30 min. Then, sections were incubated with blocking solution containing 10% normal serum goat in saline phosphate buffer, pH 7.4, for 1 hr. nNOS, iNOS, and nitrotyrosine immunoreactivities were detected using polyclonal rabbit antibodies at dilutions of 1:3,000, 1:2,500, and 1:1,000, respectively, with antibodies produced at the Cajal Institute (Uttenthal et al., 1998; Rodrigo et al., 2001; Alonso et al., 2002). Tyrosine hydroxylase (TH) was detected with a specific mouse monoclonal IgG (Sigma, St. Louis, MO) at a 1:25 dilution, and glial fibrillary acidic protein (GFAP) was detected with a specific monoclonal mouse antibody (1:500 dilution; Sigma). All antibodies were incubated overnight at 0–4°C, and their specificity was corroborated in adjacent sections by omission of primary antibodies. In addition, specificity of antibodies against nNOS, iNOS, and nitrotyrosine had been previously demonstrated (Uttenthal et al., 1998; Rodrigo et al., 2001; Alonso et al., 2002). Immunoreactivity was visualized with goat anti-rabbit IgG (1:100; Sigma), developed with the PAP system (Sigma) and 0.03% 3,3′-diaminobenzidine (Sigma), 3% nickel ammonium sulfate, and 0.01% hydrogen peroxide diluted in 0.1 M buffer acetate, yielding a black product. Sections were dehydrated with an increasing alcohol series, cleared in xylene, and coverslipped. After an overnight incubation with specific primary antibodies, colocalization studies were performed by immunofluorescence technique using FITC anti-mouse IgG coupled (1:300; Sigma) and rhodamine anti-rabbit IgG coupled (1:300; Sigma). DAPI (1:1,000; Sigma) was used as nuclear counterstain.

SDS-PAGE and Western Blotting

PA, HYP, and CTL animals 15, 21, 30, and 60 days of age (PND15, PND21, PND30, and PND60, respectively) were deeply intraperitoneally anaesthetized with cloral hydrate 28% P/V (0.1 ml/100 g body weight), sacrificed by decapitation, and enucleated. Then, anterior segments of the eyes, including the lense, were discarded and the retinas dissected, frozen, and stored at –80°C until use. Tissues were homogenized (1:3, w/v) in HEPES buffer [20 mM N-(2-hydroxethyl)piperazine-N?-(2-ethanesulfonic acid), pH 7.2, containing 0.2 M sucrose, 1 mM EDTA, 5 mM dithiothreitol, 10 μg/ml soybean trypsin inhibitor, 10 μg/ml leupeptin, 2 μg/ml pepstatin, and 0.1 mM phenylmethylsulfonyl fluoride]. All procedures were carried out at 4°C. Homogenates were centrifuged 1 hr at 105,000*g* and the supernatants collected. To use similar amounts of proteins from each sample (25 μg), protein concentration was determined by the Bradford method (Bradford, 1976), using bovine serum albumin as standard. Then, samples of supernatants were mixed 1:1 with sample buffer [10 ml Tris-HCl 0.5 M, pH 6.8, 16 ml sodium dodecyl sulfate (SDS) 10% (w/v), 8 ml glycerol, 2 ml 2-mercaptoethanol, and 0.2 ml bromophenol blue 0.1% (w/v)] and heated for 3 min at 95°C. Samples were run on an SDS-polyacrylamide gel (10% running gel with 3.5% stacking gel), with 0.25 M Tris-glycine, pH 8.3, as the electrolyte buffer, in a Bio-Rad Mini-Protein II (Bio-Rad, Madrid, Spain). Kaleidoscope Prestained Standards (Bio-Rad) were used as molecular weight markers. For Western blot analysis, proteins were transferred at 1.5 mA/cm^2 for 1 hr onto 0.2-mm polyvinylidene difluoride (PVDF) membranes (Immobilon-P; Millipore, Bedford, MA) by a semidry transfer (Bio-Rad). For protein identification, membranes were incubated overnight at 4°C with antinitrotyrosine antibody at a 1:1,000 dilution, for nNOS with the antibody at a 1:1,000 dilution, and for iNOS with the

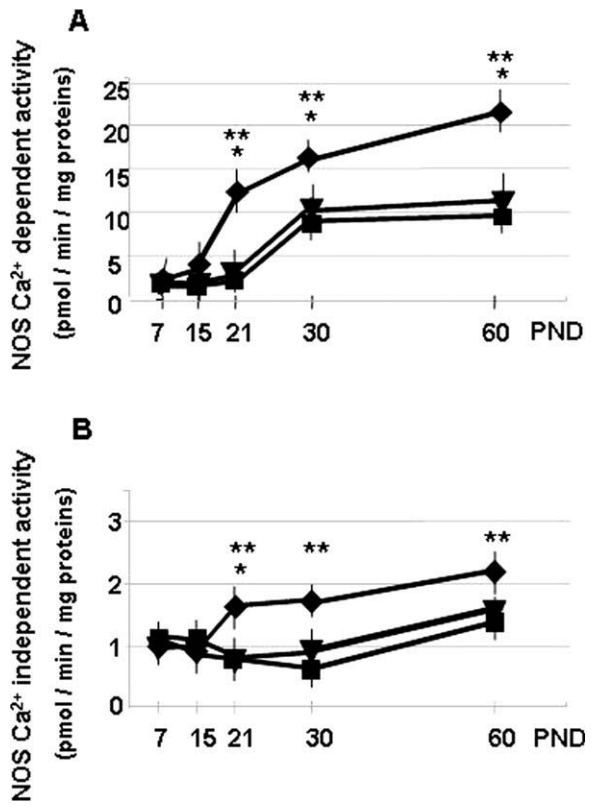

Fig. 1. Increase in NOS activity in PA according to age. A significant increase was observed for NOS Ca^{2+}-dependent and -independent activities according to age (**A** and **B**, respectively). The PA group showed a significant increase according to age from PND21 up to PND60 for both NOS isoforms, whereass, only at NOS Ca^{2+}-dependent activity, CTL and HYP showed a later significant increase, beginning on PND30. The retinas from the PA group showed a significant increase with respect to CTL in both NOS isoforms from PND21 up to PND60. The HYP group did not show significant alterations related to CTL activity. Squares, CTL; l;ozenges, PA; triangles, HYP. *Significant increase at PA vs. the PA younger group, $F_{2,15} = 14.3$, $P < 0.05$. **Significant between PA and CTL, $F_{2,15} = 11.8$, $P < 0.001$. PND, postnatal day.

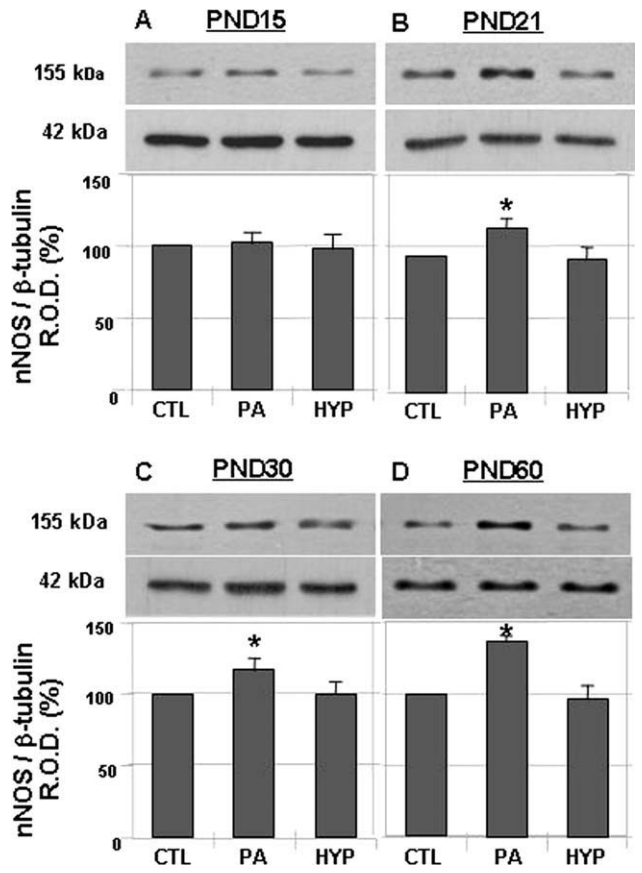

Fig. 2. nNOS protein expression is increased by perinatal asphyxia. A significant increase in nNOS expression was observed on Western blot in PA rats with respect to CTL on PND21, PND30, and PND60 (**B–D**, respectively), while no changes were observed at a younger age (**A**). HYP prevented the alterations in nNOS expression. No changes were observed in HYP with respect to CTL at any age studied (A–D). Representative Western blot images of nNOS and β-tubulin are shown at each age. nNOS R.O.D. was standardized by β-tubulin R.O.D. Graphics represent the mean ± standard deviation of four similar assays. *Statistically significant differences vs. CTL, $F_{2,15} = 23.4$, $P < 0.05$. PND, postnatal day, R.O.D., relative optical density.

antibody at a 1:2,000 dilution. To standarize the results, monoclonal IgG anti-β-tubulin (Sigma; at a 1:10,000 dilution) was used in the same membranes. To develop immunoreactivity, membranes were incubated with anti-rabbit chemiluminescence labelled IgG (GE Biosciences, Miami, FL) and exposed to X-ray blue films (CEA, Strängnäs, Sweden). Developed films were scanned with a computer-assisted densitometer (Bio-Rad, GS-800) and optical density quantified by NIH Scion Image software.

Image Analysis

Six retinal sections from five animals of each experimental group were analyzed. Care was taken with selecting anatomically matched areas of retina among animals before assays. Relative optical density (R.O.D.), cellular area (C.A.), and number of immunoreactive cells were analyzed using an Olympus BH2 microscope attached to a video camera (CCD Sony-XC77) and coupled to a computer equipped with a video card (Data Translation). Immunoreactivity used to analyze R.O.D., C.A., and number of immunopositive cells was evaluated in Scion Image software (developed by Wayne Rasband, 1995, NIH, Research Services Branch, NIMH, Bethesda, MD). R.O.D. was calculated with a gray scale of 255 gray levels. To avoid external variations, all images were taken on the same day and under the same light. The number of cells was measured in the retina segments 160 μm in length. Four segments were measured in each retinal section. Because immunohistochemistry and Western blotting are semiquantitative techniques, R.O.D. values were expressed as percentage of change respect to the CTL group, considering CTL's R.O.D. as 100%.

Statistical Analysis

Values are expressed as mean ± standard deviation. At least two similar separate experiments were evaluated in all cases. Twelve sections from each animal were analyzed. Results were evaluated by using one-way ANOVA, and comparisons

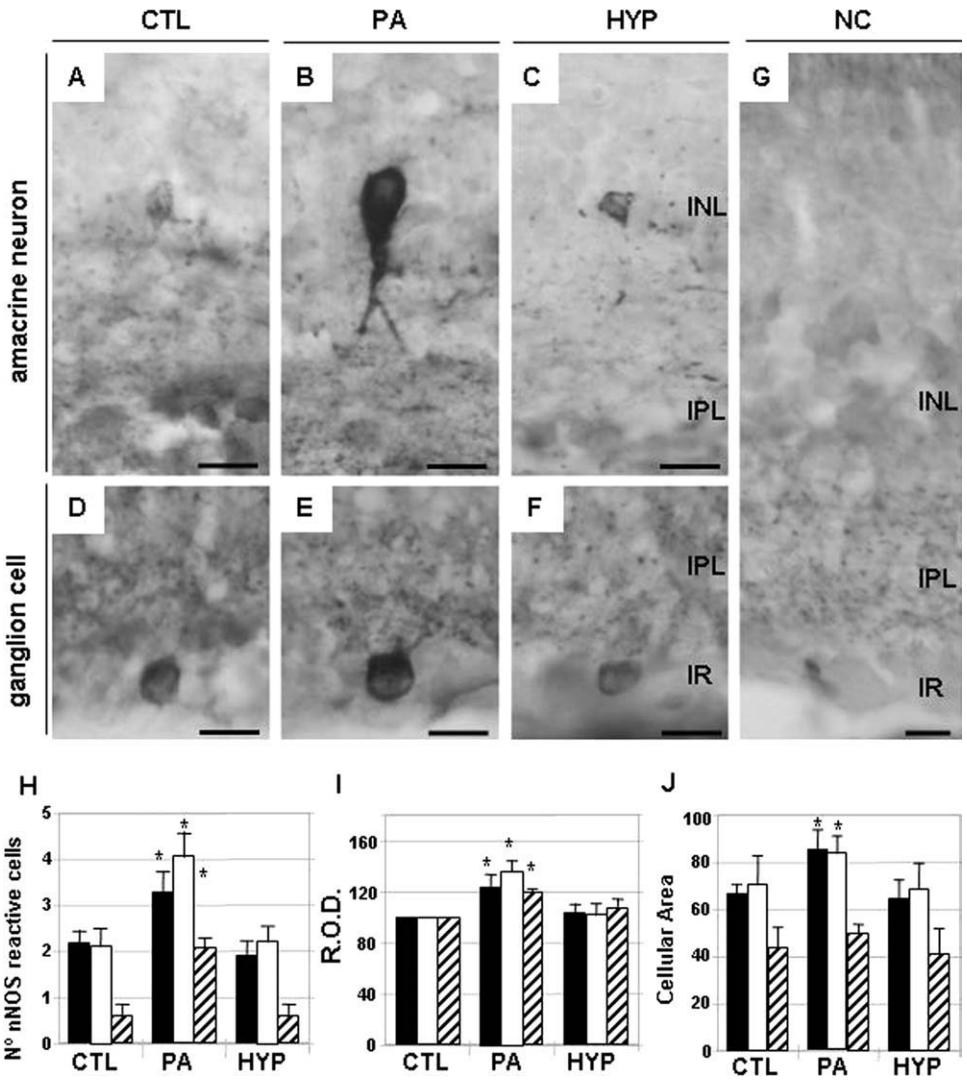

Fig. 3. Perinatal asphyxia induces significant changes at PND21 retina cells. **A–F**: Representative images of nNOS immunoreactivity in amacrine neurons and ganglion cells in retinas of CTL, AP, and HYP-PND21. A–C: Amacrine neurons. **D–F**: Ganglion cells. **G**: Negative control (NC). INL, inner nuclear layer; IPL, inner plexiform layer; IR, inner retina. **H–J**: nNOS immunoreactivity in amacrine, horizontal, and ganglion cells of the PA-PND21 group significantly increased their number (H), R.O.D. (I) and cellular area (J) with respect to CTL-PND21 tissues, with the following values. Number of nNOS immunoreactive cells = amacrine neurons: CTL, 2 ± 0.2 cells; PA, 4 ± 0.2 cells ($F_{2,15}$ = 30.4, P = 0.03); ganglion neurons: CTL, 2 ± 0.2 cells; PA, 3.5 ± 0.2 cells ($F_{2,15}$ = 55.3, P = 0.01); horizontal neurons: CTL, 0.6 ± 0.2 cells; PA, 2 ± 0.2 cells ($F_{2,15}$ = 28.7, P = 0.04); R.O.D. = amacrine neurons: PA, 23% ± 2%; ganglion neurons: PA, 40% ± 5%, horizontal neurons: PA, 21% ± 1%; *Statistically significant differences with respect to CTL, $P < 0.05$. Cellular area (μm^2) = amacrine neurons: PA, 38% ± 6% ($F_{2,15}$ = 30.8, P = 0.04); ganglion neurons: PA: 21% ± 5% ($F_{2,15}$ = 31.2, P = 0.045); horizontal neurons: PA, 5% ± 2% compared with CTL. *Statistically significant differences with respect to CTL. HYP-PND21 did not show changes vs. CTL-PND21. Solid bars, amacrine neurons; open bars, ganglion cells; hatched bars, horizontal cells. Scale bars = 15 μm.

between groups were made by Fisher's, Scheffe's, and Bonferroni-Dunn tests in GraphPad software (GraphPad Software, San Diego, CA). Differences were considered significant at $P < 0.05$.

RESULTS

Induction of NOS Activity by Perinatal Asphyxia

The time course of NOS activity in the retina of perinatal asphyctic animals 7, 15, 21, 30, and 60 days of age (PND7, PND15, PND21, PND30, and PND60, respectively) was determined. A significant time course increase was observed in NOS Ca^{2+}-dependent activity of the PA groups, from PND21 up to PND60 (Fig. 1A). The CTL and HYP groups also showed significant increases of NOS Ca^{2+}-dependent activity at PND30 and PND60 with respect to PND21 (CTL-PND30: 331 ± 11%, CTL-PND60: 362 ± 15%, HYP-PND30: 385 ± 25%, HYP-PND60: 367 ± 19%; Fig. 1A). Moreover, in

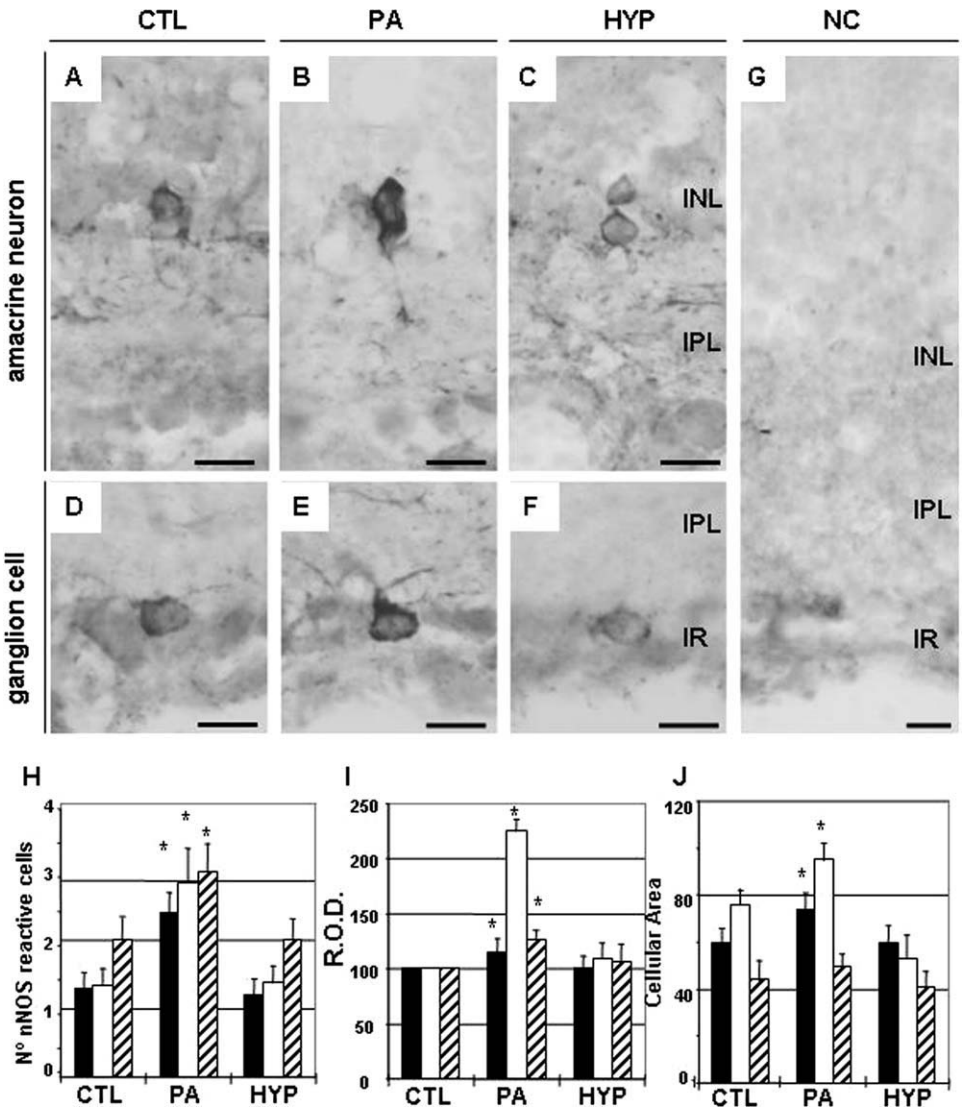

Fig. 4. Perinatal asphyxia induces significant changes at PND60 retina cells. **A–F**: Representative images of nNOS immunoreactivity in amacrine neurons and ganglion cells in retinas of CTL-, AP-, and HYP-PND60. A–C: Amacrine neurons. D–F: Ganglion cells. **G**: Negative control (NC). INL, inner nuclear layer, IPL, inner plexiform layer, IR, inner retina. **H–J**: nNOS immunoreactivity in amacrine, horizontal, and ganglion cells of the PA-PND60 group significantly increased their number (H), R.O.D (I), and cellular area (J) with respect to CTL-PND60 tissues with the following values. Number of nNOS immunoreactive cells = amacrine neurons: CTL, 1.4 ± 0.2 cells; PA, 2.5 ± 0.2 cells ($F_{2,15}$ = 30.4, P = 0.03); ganglion neurons: CTL, 1.5 ± 0.2 cells; PA, 3 ± 0.5 cells ($F_{2,15}$ = 55.3, P = 0.01); horizontal neurons: CTL, 2 ± 0.2 cells; PA, 3.2 ± 0.4 cells ($F_{2,15}$ = 28.7, P = 0.04); R.O.D. = amacrine neurons: PA, 20% ± 3%; ganglion neurons: PA, 125% ± 4%; horizontal neurons: PA, 25% ± 2%. *Statistically significant differences with respect to CTL, $P < 0.05$. Cellular area (μm^2) = amacrine neurons: PA, 30% ± 3% ($F_{2,15}$ = 30.8, P = 0.04); ganglion neurons: PA, 33% ± 5% ($F_{2,15}$ = 31.2, P = 0.045); horizontal neurons: PA, 5% ± 2% compared with CTL. *Statistically significant differences with respect to CTL. HYP-PND60 did not show changes respect to CTL-PND60. Solid bars, amacrine neurons; open bars, ganglion cells; hatched bars, horizontal cells. Scale bars = 15 μm.

each group (PND21, PND30, and PND60), PA induced a significant increase in NOS Ca^{2+}-dependent activity with respect to age-matched CTL groups, with increases of 490 ± 20%, 81 ± 7%, and 121 ± 11%, respectively (Fig. 1A). The HYP groups did not show significant alterations related to their age-matched CTL groups (Fig. 1A). On the other hand, NOS Ca^{2+}-independent activity showed a behavioral pattern similar to that of Ca^{2+}-dependent NOS, with a significantly increased activity induced by PA from PND21 up to PND60 with respect to PND15 (PND21: 63 ± 3%, PND30: 19 ± 4%, PND60: 90 ± 5%; Fig. 1B). Neither the CTL nor the HYP groups showed significant differences according to the age (Fig. 1B). In addition, the NOS Ca^{2+}-independent activity showed that PA induced a significant increase in each group (PND21, PND30, and PND60) compared with the age-matched CTL groups (PND21: 90 ± 7%, PND30: 131 ± 7%,

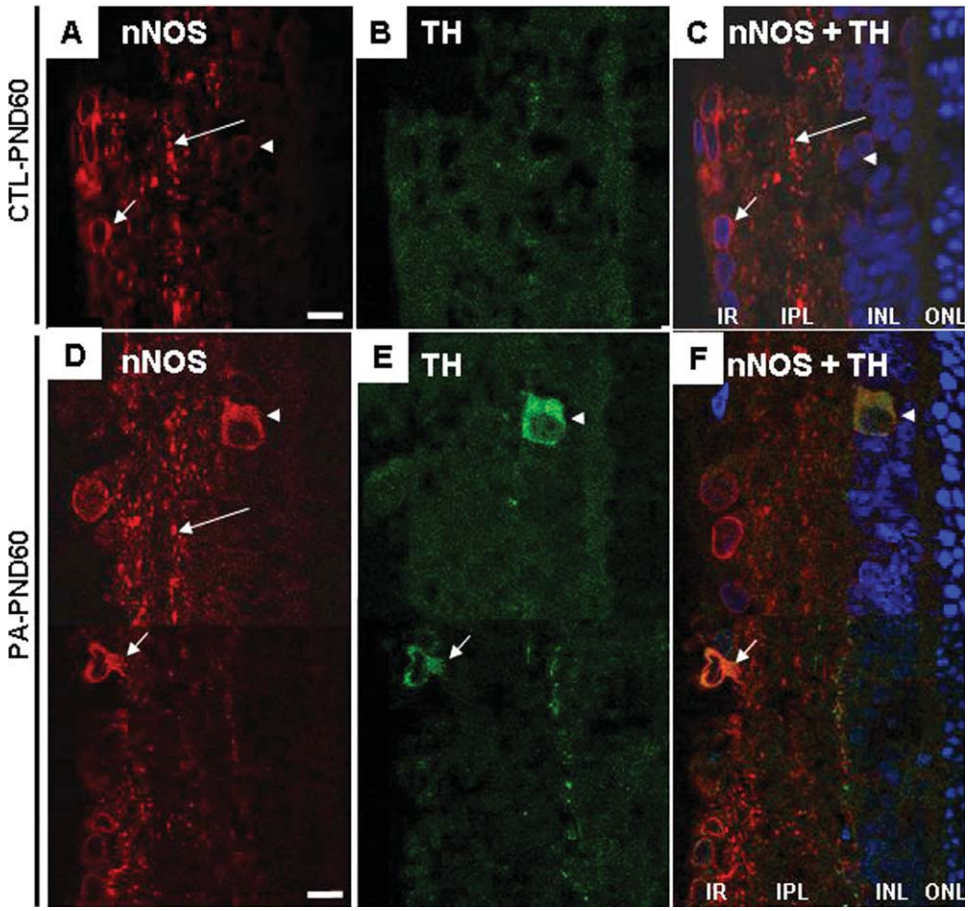

Fig. 5. nNOS immunoreactivity colocalizes with tyrosine hydroxylase in cells of the PA group. **A–C**: Representative images of retinas from the CTL-PND60 group. CTL-PND60 rats show nNOS immunoreactivity in the cytoplasm of ganglion cells (A, small arrow), amacrine neurons (A, arrowhead), and buttons of amacrine cell processes extended into the IPL (A, large arrow), while no TH immunoreactivity was observed (B). **D–F**: Representative photomontage images of retinas from PA-PND60 animals. Colocalization of nNOS and TH immunoreactivity was observed in ganglion cells (F, arrow) and amacrine neurons (F, arrowhead) of PA-PND60 rats. ONL, outer nuclear layer, INL, inner nuclear layer, IPL, inner plexiform layer, IR, inner retina. Scale bars = 15 μm. [Color figure can be viewed in the online issue, which is available at wileyonlinelibrary.com.]

PND60: 121 ± 11%; Fig. 1B). The HYP groups did not show significant alterations vs. their age-matched CTL groups (Fig. 1B).

Induction of NOS Expression by Perinatal Asphyxia

Considering the significant increase in the NOS activity in the PA retinas, we focused next on the evaluation of the effect of perinatal asphyxia on nNOS and iNOS protein expression and localization from PND15 up to PND60 rats.

Modulation of nNOS Expression by Perinatal Asphyxia

When the 155-kDa band corresponding to nNOS expression was analyzed, a significant increase of 20% ± 3% was detected for the PA-PND21 group with respect to the age-matched CTL animals (Fig. 2B). No differences were observed in HYP-PND21 animals in relation to CTL (Fig. 2B), and no alterations were observed in retinas from PND15 animals with the PA or HYP treatments (Fig. 2A). nNOS expression remained elevated in the PA group from PND21 to PND60, with a significant increase of 18% ± 2% in PND30 and 38% ± 3% in PND60 with respect to their age-matched CTL rats (Fig. 2C,D). Then, a morphometric study was developed in PND21 and PND60 animals. First, light-specific nNOS immunoreactivity was observed at the most inner layers of the retina (inner nuclear layer, inner plexiform layer, and ganglion cells layer) of CTL rats with immunolocalization in three cell types: 1) soma of amacrine neurons at the inner margin of the inner nuclear layer and at their prolongations at the inner plexiform layer, 2) ganglion neurons from the ganglion cells layer, and 3) horizontal neurons of the outer margin of the inner nuclear layer (although they showed a slight immunoreactivity; Figs. 3A, 4A). A significant increase was

observed in the number and R.O.D. of the three types of nNOS-immunoreactive cells of the retina in PA-PND21 (Fig. 3H,I) and PA-PND60 (Fig. 4H,I) rats with respect to their age-matched CTL groups. In addition, a significant increase in nNOS-immunoreactive C.A. was observed in amacrine and ganglion neurons of PA-PND21 (Fig. 3J) and PA-PND60 (Fig. 4 J) rats compared with the age-matched CTL, whereas C.A. of horizontal neurons was not altered by PA (Figs. 3J, 4J). No changes were observed in amacrine, ganglion, or horizontal neurons of HYP-PND21 and HYP-PND60 animals with respect to the age-matched CTL (Figs. 3H–J, 4H–J). Amacrine cell processes extended into the inner plexiform layer, showing buttons of nNOS immunoreactivity. PA-PND21 and PA-PND60 rats showed a significant increase in R.O.D. at the inner plexiform layer with respect to the age-matched CTL (46% ± 7% and 32% ± 5%, respectively), whereas retinas from the HYP group showed no alterations in nNOS R.O.D. at this layer at both evaluated ages. To understand the action of perinatal asphyxia on nNOS modulation, and considering that NO synthesis is regulated by dopamine (Wakakura, 2001), we evaluated the expression of TH, the enzyme responsible for dopamine synthesis, in comparison with nNOS expression. Immunofluorescence study showed colocalization of nNOS and TH in the cytoplasm of a subpopulation of ganglion and amacrine cells of PA-PND60 rats (Fig. 5F), which was not present in the CTL-PND60 group (Fig. 5C). HYP rats did not show colocalization for nNOS and TH at any of the time periods studied.

Modulation of iNOS Expression by Perinatal Asphyxia

iNOS expression in the retinas was determined by immunoblot, showing a band with a molecular weight of 135 kDa. A significant increase in iNOS expression was observed in PA-PND21 and PA-PND60 rats with respect to CTL (71% ± 14% and 76% ± 18%, respectively), whereas iNOS expression was not altered in HYP animals (Fig. 6A,B). Next, to analyze iNOS localization, an immunohistochemistry assay was developed. iNOS localization was detected in ganglion cells and Müller cell processes of the inner retina and in cells of the inner nuclear layer of the retina (Fig. 7). PA-PND21 rats showed a significant increase in iNOS R.O.D. with respect to CTL-PND21, at IR as at the inner nuclear layer (77% ± 5% and 66% ± 3%, respectively, Fig. 7A), but no alterations in HYP-PND21 rats (Fig. 7A). Similar results were observed in PND60 animals (Fig. 7B). We have recently described the presence of engrossed, tortuous, and enlarged Müller cell internal processes of the retina of PA rats with increased GFAP immunoreactivity expanded along the inner retinal layers (Rey-Funes et al., 2010). In the present work we observed iNOS localization at Müller cell internal processes at the inner retina (Fig. 7 D,H), so we decided to study iNOS and GFAP colocalization. PA-PND60 rats showed iNOS- and GFAP-immunoreactive colocalization at the inner processes

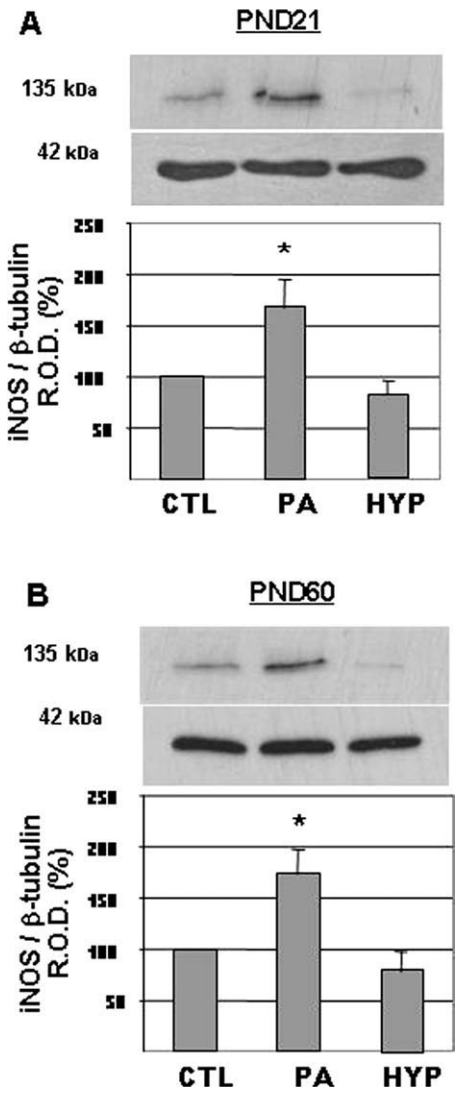

Fig. 6. iNOS protein expression is increased by perinatal asphyxia. A significant increase in iNOS expression was observed on Western blot in PA with respect to CTL, on PND21 and PND60 groups (**A** and **B**, respectively), whereas no changes were observed in HYP compared with CTL. Representative Western blot images of iNOS and β-tubulin are shown at each age. iNOS R.O.D. was standardized by β-tubulin R.O.D. Graphics represent the mean ± standard deviation of four similar assays. *Significant vs. CTL ($F2,15 = 35.8$, $P < 0.05$). PND, post natal day, R.O.D., relative optical density.

of Müller cells in the inner limiting layer (Fig. 8F), whereas CTL-PND60 animals did not show colocalization between GFAP and iNOS (Fig. 8C).

Induction of Protein Nitration by Perinatal Hypoxia

Given the increases in NOS activity induced by PA observed, we studied the retinal protein nitrated state. Diverse nitrotyrosine protein species of 84 kDa, 72 kDa, 59.5 kDa, 50 kDa, 47 kDa, and 22 kDa were detected in the immunoblot of CTL-PND60 rats (Fig. 9A). A significant increase in R.O.D. was evidenced for all nitrated

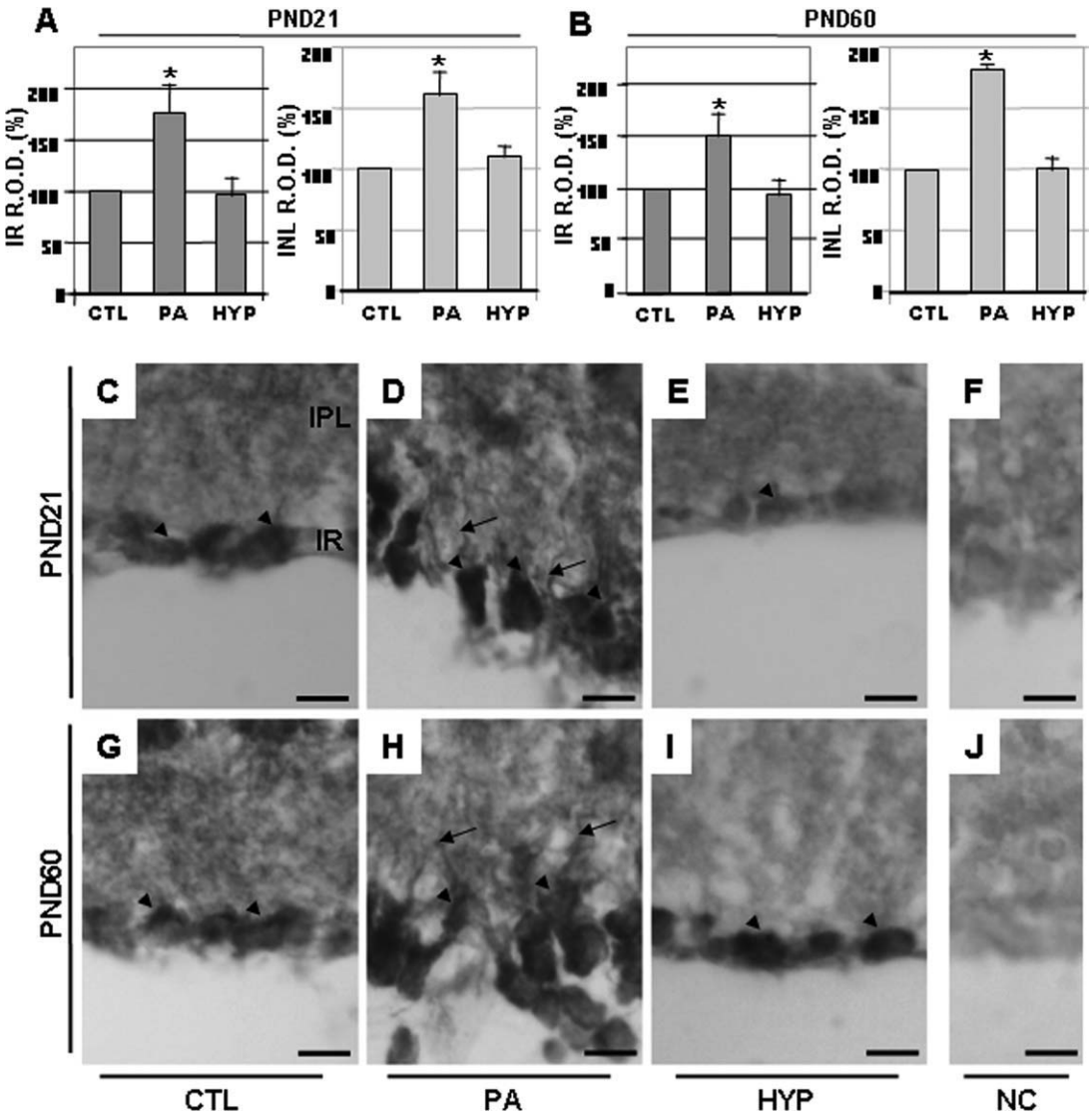

Fig. 7. Perinatal asphyxia induces significant increases in iNOS relative optical density. **A,B**: A significant increase is observed in iNOS relative optical density (R.O.D.) of ganglion cells from the inner retina (IR) and cells from the inner nuclear layer (INL) of PA-PND21 (A) and PA-PND60 (B) with respect to their corresponding CTLs, showing the following values: PA-PND21, IR 75% ± 25% increase vs. CTL ($F_{2,15} = 41.9$, $P = 0.01$); INL 65% ± 20% increase vs. CTL ($F_{2,15} = 27.9$, $P = 0.04$); PA-PND60, IR 55% ± 20% increase vs. CTL ($F_{2,15} = 67.8$, $P = 0.008$); INL; 85% ± 5% increase vs. CTL ($F_{2,15} = 9.8$, $P = 0.01$). iNOS relative optical density increases were prevented by HYP treatment, showing values similar to those of CTLs at both evaluated ages. *Statistically significant with respect to CTL. **C–J**: Representative images of iNOS immunoreactivity in ganglion cells from the inner retina (arrowhead), cells from the inner nuclear layer, and Müller cell processes in the inner plexiform layer (arrows) of PND21 (C–E) and PND60 (G–I). iNOS immunoreactivity was not observed in the Müller cell processes of the CTL or HYP groups. F,J: Negative controls (NC). INL, inner nuclear layer, IPL, inner plexiform layer, IR, inner retina. Scale bars = 15 μm.

species of retinas of the PA-PND60 group with respect to the CTL-PND60 group (Fig. 9B), whereas HYP-PND60 rats did not show significant alterations for any nitrotyrosine-immunoreactive protein species with respect to their CTL counterparts. Then, nitrotyrosine immunoreactivity and localization was determined at retinal slides. Nitrotyrosine immunoreactivity was slightly present in the inner retina of CTL animals (Fig. 10A), whereas specific immunolocalization of nitrotyrosine was observed at the inner retina, inner nuclear layer, and Müller cell internal processes of PA-PND60 rats (Fig. 10F). A time course study of nitrotyrosine expression in IR from PND21 up to PND60 PA rats showed a progressive increase in R.O.D. with a maximum level of R.O.D. in PND60 animals, but no alterations in HYP rats (Fig. 9I). Thus, in PND21, PND30, and PND60 animals, nitrotyrosine R.O.D. was significantly increased in the retinas from the PA group with respect to the age-matched CTL group, whereas HYP animals did not show changes (Fig. 9I). To study protein nitration at Müller cell internal processes in

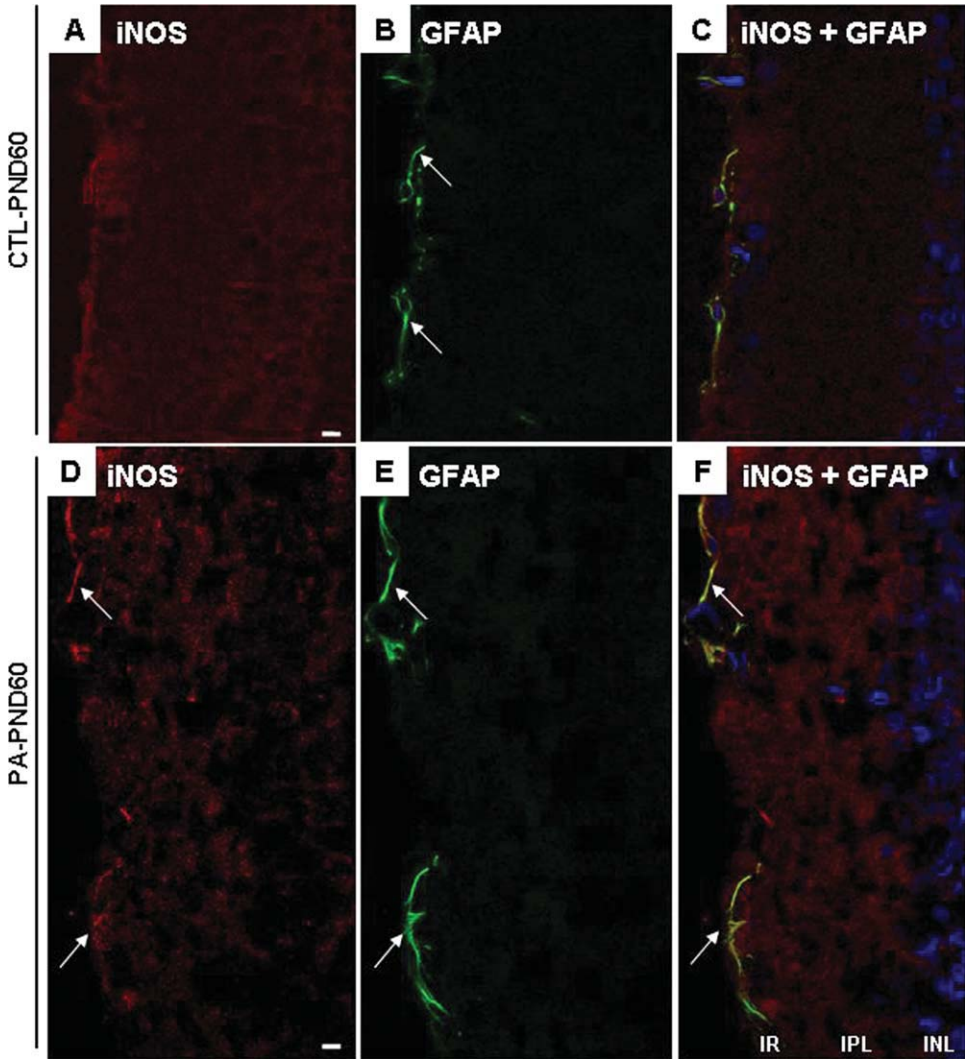

Fig. 8. iNOS immunorreactivity is observed in GFAP immunoreactive Müller cell processes in the PA group. **A–C**: Representative images of retinas from CTL-PND60 rats. GFAP immunoreactivity is observed at Müller cell processes of the inner limiting layer (B, arrows), but no iNOS immunoreactivity was observed in CTL-PND60 rats (A). **D–F**: Representative images of retinas from PA-PND60 rats. Colocalization of iNOS and GFAP immunoreactivity was observed in Müller cell processes of the inner limiting layer of the PA-PND60 group (F, arrows). INL, inner nuclear layer, IPL, inner plexiform layer, IR, inner retina. Scale bars = 15 μm. [Color figure can be viewed in the online issue, which is available at wileyonlinelibrary.com.]

the inner retina, a coimmunohistochemical study was performed. Colocalization between nitrotyrosine and GFAP was observed at Müller cell processes of the inner limiting region of PA-PND60 rats (Fig. 11F), and GFAP immunoreactivity without nitrotyrosine colocalization was observed in CTL-PND60 animals (Fig. 11B,C).

DISCUSSION

This work shows that the NO system in the retina is highly sensitive to perinatal asphyxia, inducing long-term alterations in the activity and expression of both the inducible and the constitutive NOS isoforms, predominantly at the inner margin of the retina. NOS Ca^{2+}-independent activity (corresponding to iNOS activity) was increased by asphyxia, reaching the maximum value in PND21 animals. At the same time, a significant increase in NOS Ca^{2+}-dependent activity was induced by asphyxia with progressive increases according to age. Although NOS Ca^{2+}-dependent activity corresponds to both nNOS and eNOS isoforms, we focused our work on studying nNOS expression, which shows long-term response to hypoxia-ischemia involved in IPR development and second phase of ROP, in contrast, eNOS is expressed as acute response after ischemic-hypoxic events inducing NO delivery to increase vasodilatation, which is not the aim of the present research.

The study of nNOS and iNOS expression showed that cells of the most inner layers of the retina were more sensitive to oxygen deprivation, with specific retinal cell

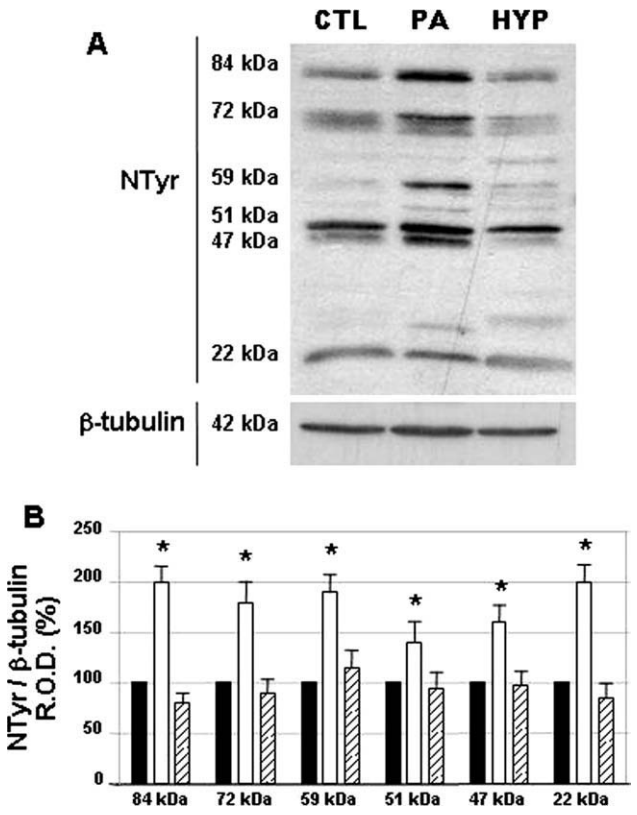

Fig. 9. Perinatal asphyxia induces an increase in nitrated proteins in the retina. **A**: Six different nitrotyrosine protein species were observed in retinas on Western blot. Representative Western blot images of nitrotyrosine and β-tubulin for PND60 retinas. β-Tubulin was quantified to standardize the nitrotyrosine results. **B**: Significant increases were observed for all nitrated protein species of the PA group respect to CTL. No changes were observed for the HYP group. Graphic represent the mean ± standard deviation of four similar assays. Nitrotyrosine R.O.D. was standardized by β-tubulin R.O.D. at each nitrotyrosine protein species. ⋆Statistically significant with respect to CTL ($P < 0.001$). Solid bars, CTL; hatched bars, PA; open bars, HYP.

type localization according to the isoform. nNOS was specifically localized in amacrine, horizontal, and ganglion neurons of the inner layers of the retina, whereas iNOS was identified in ganglion cells, Müller cell processes, and somas of cells of the inner nuclear layer. Although similar observations had been previously described by others (Kobayashi et al., 2000; Eldred and Blute, 2005), here we show significant alterations in R.O.D., C.A., and the number of these NOS-immunoreactive cells, with significant increases induced by perinatal asphyxia.

A time course study of animals from PND7 up to PND60 perinatally exposed to asphyxia showed that both retinal nNOS and iNOS significantly increased their activity in the retinas of 21-day-old animals, as a consequence, at least in part, of a significant increase in their cellular expression. However, NOS activity appears to develop its own time course pattern according to the tissue. Other tissues such as brain or spinal cord show a different pattern of NOS activity, with significant increases induced by hypoxia at early postnatal stages (between 1 and 7 days old) and a significant decline thereafter (Castro-Blanco et al, 2003; Fernández et al., 2003; Dorfman et al., 2009). Nevertheless, in our work, this change remained increased up to PND 60, also showing significant increases in nNOS with respect to younger animals.

NO is postulated to be one of the most relevant neurotoxic factors, increasing in the central nervous system as a consequence of hypoxia-ischemia, including the retina (Osborne et al., 2004). An increment in glutamate activity induces NMDA activation, which increases the Ca^{2+} inflow that activates NOS. The resultant NO increment induces protein nitration, resulting in apoptosis (Sennlaub et al., 2002). In this study, nitrotyrosine immunoreactivity, used as a marker of protein nitration, was shown to increase from PND21 to PND60. This was expected according to the increase observed in NOS activity. A significant increase in six species of nitrated proteins varying in size from 22 up to 84 kDa was observed in the retinas of PA-PND60 animals. These observations are consistent with previous reports that describe an increase in several nitrated proteins in the spinal cord subjected to perinatal asphyxia (Dorfman et al., 2009) and in the brains of rats subjected to hypoxia during delivery (Fernandez et al., 2003; van den Tweel et al., 2005a). However, these tissues presented a different pattern of nitrated protein species, showing that the protein sensitivity to NO increase is related to the tissue. The increased production of NO observed may change the normal cell metabolism by a neurotoxic effect, by altering the catalytic activity of many enzymes, changing structural proteins that increase proteolysis (Bartosz, 1996) and apoptosis (Palluy and Rigaud, 1996; Sennlaub et al., 2002) and contributing to retinal damage. In a recent report (Rey-Funes et al., 2010), we described alterations in Müller cells in the retinas of PA animals with enlarged, tortuous, and engrossed internal processes, resulting in increased thickness of the glial inner limiting layer. In the present work, GFAP localization was studied in relation to iNOS and nitrotyrosine expression, and a specific colocalization of GFAP with these markers was observed. A significant increase in a 51-kDa nitrated protein species that may correspond to GFAP was observed. Further experiments should be developed to confirm this presumption.

When hypothermia was applied, it proved to be protective against damage of the retina induced by perinatal asphyxia, inhibiting all alterations of both NOS isoforms and nitration of proteins. Hypothermia has proved to be protective against the development of long-term NOS alterations in the central nervous system (CNS; Dorfman et al. 2009, Loidl et al., 1998, 2000, Herrera-Marschitz et al., 1993) and the present work extends these observations to the retina. Several other strategies such as the use of antioxidants (Raju et al., 1997), D-penicillamine (Phelps et al., 2000), allopurinol (Russell and Cooke, 1995), indomethacin (Nandgaunkar et al., 1999), dexamethasone (Rotschild et al., 1999), or rofecoxib (Wilkinson-Berka

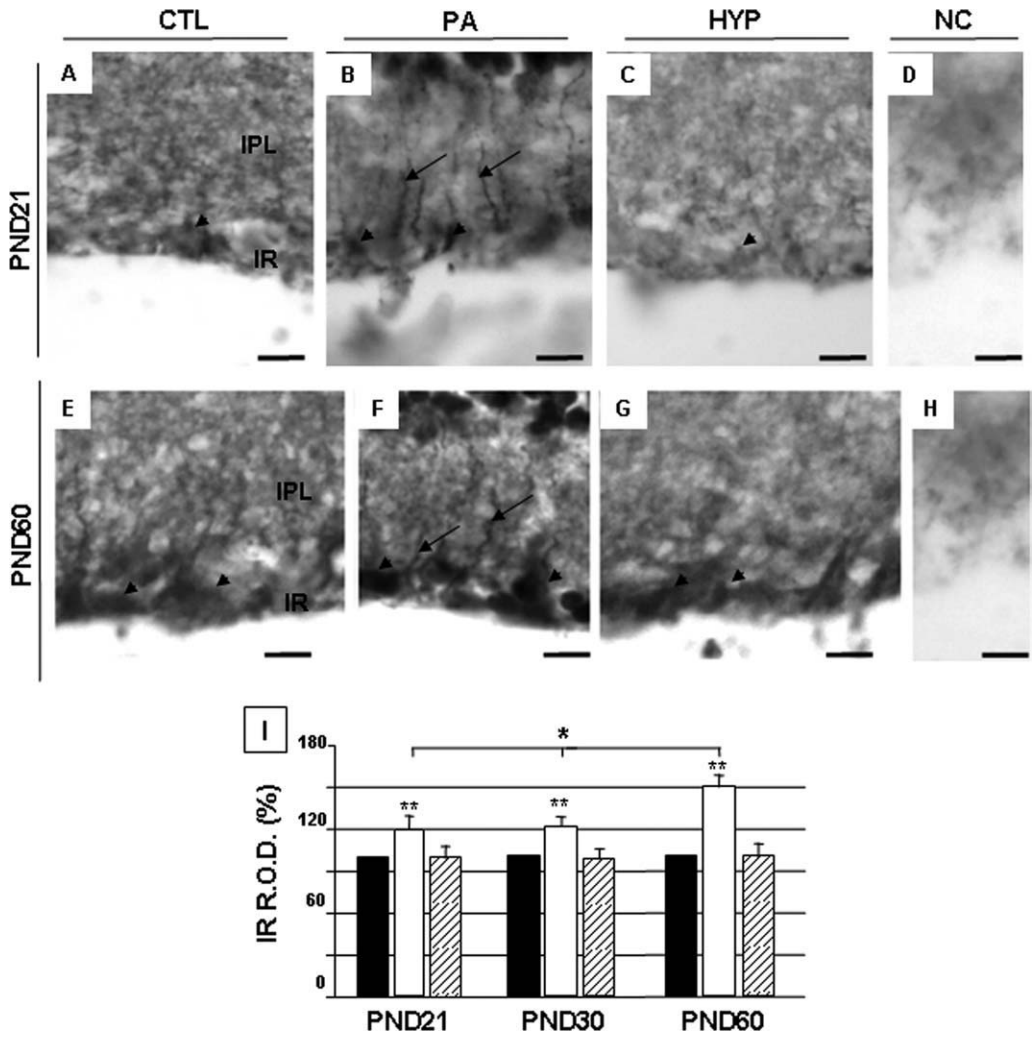

Fig. 10. PA increases nitrotyrosine expression in the retina. **A–H**: Representative images of nitrotyrosine immunoreactivity in the retinas from PND21 (A–D) and PND 60 (E–H) of CTL (A,E), PA (B,F), and HYP (C,G) animals. D,H: Negative controls (NC). Nitrotyrosine immunoreactivity was observed in the ganglion cells (arrowheads) of the three groups and in the Müller cells processes in the IPL of PA group only (arrows). **I**: Significant increase was observed in the R.O.D. of nitrotyrosine at IR of PA group with respect to CTL at PND21, PND30, and PND60 (double asterisks, PA-PND21: 33% ± 10%, $F_{2,15} = 27.1$, $P = 0.03$; PA-PND30: 35% ± 5%, $F_{2,15} = 107.1$, $P = 0.001$; PND60: 66% ± 10%, $F_{2,15} = 33.2$, $P = 0.02$). Moreover, significant increase was observed for the R.O.D. of nitrotyrosine of the PA group according to age with a 50% increase in PA-PND60 respect to PA-PND21 and PND30 (single asterisk, $P < 0.05$). No changes were observed in the HYP group. Solid bars, CTL; hatched bars, PA; open bars, HYP. Scale bars = 15 μm.

et al., 2003), as well as early light reduction (Phelps and Watts, 1997) or oxygen supplementation (STOP ROP Multicenter Trial, 2000), have been tried in order to prevent hypoxia-ischemia injury. However, only a small decrease in ROP severity was obtained (Howlett, 2003). In contrast, the decrease in environmental temperature at birth is an efficient therapeutic tool for preventing IPR development (Blackstone et al., 2005; Carey et al., 2003).

The present model of perinatal asphyxia may thus be useful in studying different kinds of ophthalmologic pathologies, including several degrees of IPR. Recently, we have shown that the actual scheme of perinatal asphyxia leads to severe signs of retinopathy that are compatible with pathological descriptions of ROP (Rey-Funes et al., 2010). Another advantage of the present experimental model of global hypoxia-ischemia is that it offers the possibility of studying the long-term effects of perinatal asphyxia, because the newborn pups are left to grow with surrogated mothers. Preperipartum pathological situations, as well as untoward obstetric maneuvers, are accompanied by different degrees of oxygen deprivation at birth, IPR being a frequent consequence. Because the development of the CNS of rats at the moment of delivery is equivalent to that of humans at 32 weeks of gestation (Palmer and Vannucci, 1993), the present model offers the possibility of studying and comparing the alterations in the CNS with those in humans produced by prematurity.

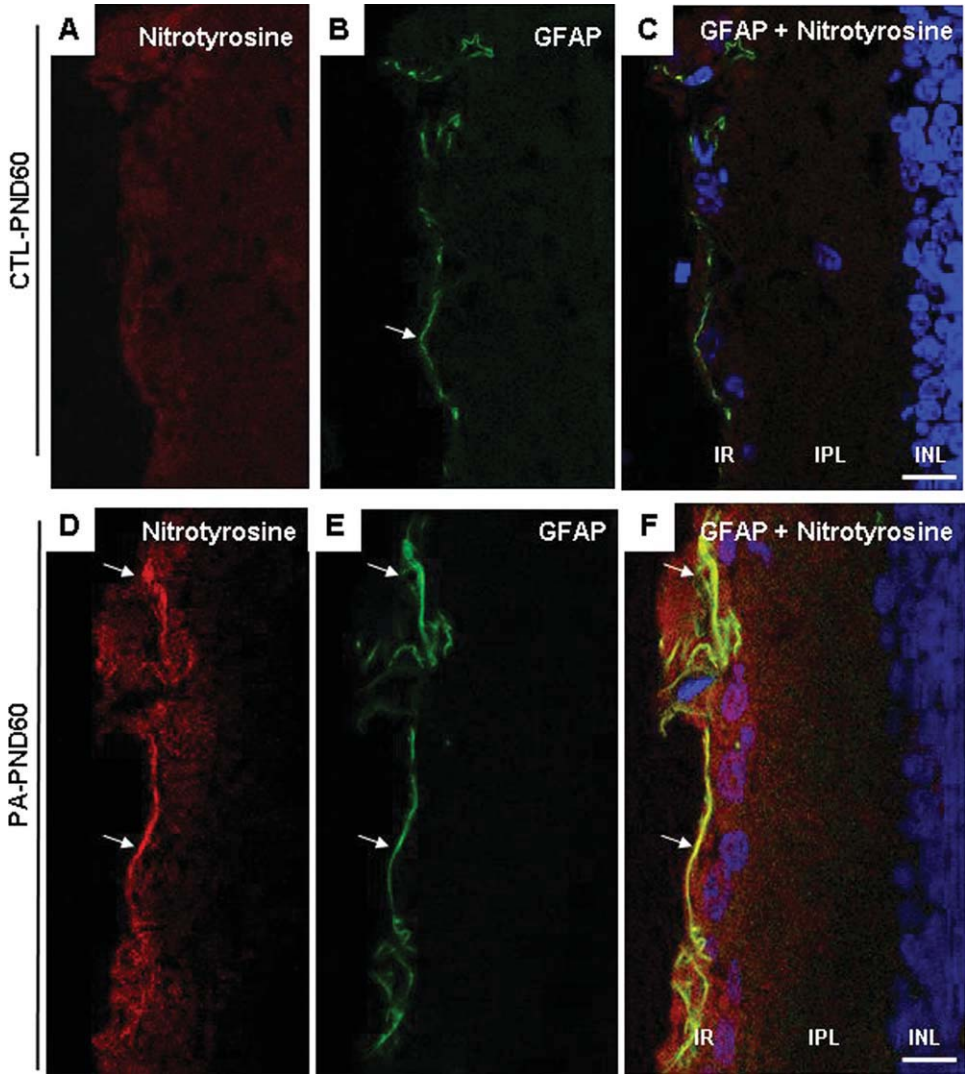

Fig. 11. Nitrotyrosine immunorreactivity is observed in GFAP-immunoreactive Müller cell processes in the PA group. **A–C**: Representative images of retinas from CTL-PND60 rats. GFAP immunoreactivity was observed at Müller cell processes of the inner limiting layer (B, arrow), but no nitrotyrosine immunoreactivity was observed in CTL-PND60 rats (A). **D–F**: Representative images of retinas from PA-PND60 rats. Colocalization of nitrotyrosine and GFAP immunoreactivity was observed in Müller cell processes of the inner limiting layer of the PA-PND60 group (F, arrows). INL, inner nuclear layer, IPL, inner plexiform layer, IR, inner retina. Scale bars = 15 μm. [Color figure can be viewed in the online issue, which is available at wileyonlinelibrary.com.]

In conclusion, here we show that hypoxia-ischemia induces alterations in the nitric oxide system. The model of perinatal asphyxia used in the present research has proved useful for the study of IPR development, including the second phase of ROP (Rey-Funes et al., 2010). Considering that, at the retina, neurotoxicity induced by hypoxia is related, at least in part, to alterations in the nitric oxide system (Osborne et al, 2004), we speculate that the observed alterations in the NO system may be involved in IPR development. Further mechanistic studies should be carried out to investigate and demonstrate NO's direct responsibility in the physiopathological alterations observed at hypoxic-ischemic retinas. The present model contributes valuable information for unraveling the physiopathological mechanisms of retinal diseases and may allow the application of possible therapeutic strategies to prevent them. The hypothermic treatment applied in the present study during the temporal window while asphyxia was induced is an effective therapy and could be adapted and translated into the clinic as an efficient tool for preventing the development of retinal neural damage resulting from global hypoxia-ischemia.

ACKNOWLEDGMENTS

We thank Ms. Africa Sandonis Consuegra and Mr. Etelvino Sánchez Pastor for their excellent technical assistance.

REFERENCES

Alonso D, Serrano J, Rodriguez I, Ruiz-Cabello J, Fernández AP, Encinas JM, Castro-Blanco S, Bentura ML, Santacana M, Richart A, Fernández-Vizarra P, Uttenthal LO, Rodrigo J. 2002. Effects of oxygen and glucose deprivation on the expression and distribution of neuronal and inducible nitric oxide synthases and on protein nitration in rat cerebral cortex. J Comp Neurol 443:183–200.

American Psychiatric Association. 1987. Diagnosis and statistical manual of mental disorders (DSM III),3rd ed. Washington, DC: American Psychiatric Association.

Bartosz G. 1996. Peroxynitrite mediator of the toxic action of nitric oxide. Acta Biochem Pol 43:645–659.

Battin MR, Penrice J, Gunn TR, Gunn AJ. 2003. Treatment of term infants with head cooling and mild systemic hypothermia (35.0 degrees C and 34.5 degrees C) after perinatal asphyxia. Pediatrics 111:244–251.

Beckman JS. 1990. Ischaemic injury mediator. Nature 345:27–28.

Beckman JS. 1996. Oxidative damage and tyrosine nitration from peroxynitrite. Chem Res Toxicol 9:836–844.

Blackstone E, Morrison M, Roth MB. 2005. H2S induces a suspended animation-like state in mice. Science 308:518.

Bradford MM. 1976. A rapid and sensitive method for the quantitation of microgram quantities of protein utilizing the principle of protein-dye binding. Anal Biochem 72:248–254.

Bredt DS, Snyder SH. 1992. Nitric oxide, a novel neuronal messenger. Neuron 8:3–11.

Carey HV, Andrews MT, Martin SL. 2003. Mammalian hibernation: cellular and molecular responses to depressed metabolism and low temperature. Physiol Rev 83:1153–1181.

Castro-Blanco S, Encinas JM, Serrano J, Alonso D, Gómez MB, Sánchez J, Ríos-Tejada F, Fernández-Vizarra P, Fernández AP, Martínez-Murillo R, Rodrigo J. 2003. Expression of nitrergic system and protein nitration in adult rat brains submitted to acute hypobaric hypoxia. Nitric Oxide 8:182–201.

Chemtob S, Hardy P, Abran D, Li DY, Peri K, Cuzzani O, Varma DR. 1995. Peroxide–cyclooxygenase interactions in postasphyxial changes in retinal and choroidal hemodynamics. J Appl Physiol 78:2039–2046.

Clancy RR, Sladky JT, Rorke LB. 1989. Hypoxic-ischemic spinal cord injury following perinatal anoxia. Ann Neurol 25:185–189.

Crofts BJ, King R, Johnson A. 1998. The contribution of low birth weight to severe vision loss in a geographically defined population. Br J Ophthalmol 82:9–13.

Cunningham RG, Leveno KJ, Ploom SL, Gilstrap LC, Hauth JC, Wendstrom KD. 2005. Williams obstretics,22nd ed. New York: Mc Graw-Hill.

Dawson TM, Bredt DS, Fotuhi M, Hwang PM, Snyder SH. 1991. Nitric oxide synthase and neuronal NADPH diaphorase are identical in brain and peripneral tissues. Proc Natl Acad Sci U S A 88:7797–7801.

Dorfman VB, Lopez-Costa JJ, Vega C, Bayona JC, Capani F, Fabian Loidl C, Coirini H. 2004. Changes of NADPH-diaphorase reactivity in lumbar spinal cord of short-term streptozotocin induced diabetic rats. Brain Res 997:185–193.

Dorfman VB, Rey-Funes M, Bayona JC, López EM, Coirini H, Loidl CF. 2009. Nitric oxide system alteration at spinal cord as a result of perinatal asphyxia is involved in behavioral disabilities: hypothermia as preventive treatment. J Neurosci Res 87:1260–1269.

Ekimova IV. 2003. Changes in the metabolic activity of neurons in the anterior hypothalamic nuclei in rats during hyperthermia, fever, and hypothermia. Neurosci Behav Physiol 33:455–460.

Eldred WD, Blute TA. 2005. Imaging of nitric oxide in the retina. Vis Res 45:3469–3486.

Fernández AP, Alonso D, Lisazoaín I, Serrano J, Leza JC, Bentura ML, López JC, Encinas JM, Fernández-Vizarra P, Castro-Blanco S, Martínez A, Martinez-Murillo R, Lorenzo P, Pedrosa JA, Peinado MA, Rodrigo J. 2003. Postnatal changes in the nitric oxide system or the rat cerebral cortex after hypoxia during delivery. Brain Res Dev Brain Res 142:177–192.

Gisselsson LL, Matus A, Wieloch T. 2005. Actin redistribution underlies the sparing effect of mild hypothermia on dendritic spine morphology after in vitro ischemia. J Cereb Blood Flow Metab 25:1346–1355.

Goureau O, Hicks D, Courtois Y. 1994. Human retinal pigmented epithelial cells produce nitric oxide in response to cytokines. Biochem Biophys Res Commun 198:120–126.

Gunn AJ. 2000. Cerebral hypothermia for prevention of brain injury following perinatal asphyxia. Curr Opin Pediatr 12:111–115.

Hardy P, Peri KG, Lahaie I, Varma DR, Chemtob S. 1996. Increased nitric oxide synthesis and action preclude choroidal vasoconstriction to hyperoxia in newborn pigs. Circ Res 79:504–511.

Hardy P, Dumont I, Bhattacharya M, Hou X, Lachapelle P, Varma DR, Chemtob S. 2000. Oxidants, nitric oxide and prostanoids in the developing ocular vasculature: a basis for ischemic retinopathy. Cardiovasc Res 47:489–509.

Herrera-Marschitz M, Loidl CF, Andersson K, Ungerstedt U. 1993. Prevention of mortality induced by perinatal anoxia: hypothermia or glutamate antagonism? Amino Acids 5:413–419.

Hill A. 1991. Current concepts of hypoxic-ischemic cerebral injury in the term newborn. Pediatr Neurol 7:317–325.

Howlett A. 2003.Study of prematures with RDS treated with inositol. Cochrane Library, Issue 1.

Jankov RP, Negus A, Tanswell AK. 2001. Antioxidants as therapy in the newborn: some words of caution. Pediatr Res 50:681–687.

Katz LM, Young AS, Frank JE, Wang Y, Park K. 2004. Regulated hypothermia reduces brain oxidative stress after hypoxic-ischemia. Brain Res 1017:85–91.

Kobayashi M, Kuroiwa T, Shimokawa R, Okeda R, Tokoro T. 2000. Nitric oxide synthase expression in ischemic rat retinas. Jpn J Ophthalmol 44:235–244.

Koppal T, Drake J, Yatin S, Jordan B, Varadarajan S, Bettenhausen L, Butterfield DA. 1999. Peroxynitrite-induced alterations in synaptosomal membrane proteins: insight into oxidative stress in Alzheimer's disease. J Neurochem 72:310–317.

Lei B, Adachi N, Arai T. 1997. The effect of hypothermia on H_2O_2 production during ischemia and reperfusion: a microdialysis study in the gerbil hippocampus. Neurosci Lett 222:91–94.

Loidl CF. 1997.Short and long term effects of perinatal asphyxia. Thesis, Maastricht University, The Netherlands.

Loidl CF, Herrera-Marschitz M, Andersson K, You Z-B, Goiny M, O'Connor WT, Bjelke B, Ungerstedt U. 1993. Short and long-term effects of perinatal asphyxia in rats monitored with peripheral and intracerebral microdialysis. Amino Acids 5:167.

Loidl CF, Herrera-Marschitz M, Andersson K, You Z-B, Goiny M, O'Connor WT, Silveira R, Rawal R, Bjelke B, Chen Y, Ungerstedt U. 1994. Long-term effects of perinatal anoxia on basal ganglia neurotransmitter systems studied with microdialysis in the rat. Neurosci Let 175:9–12.

Loidl CF, De Vente J, Markerink van Ittersum M, Van Dijk EH, Vles JS, Steinbusch H, Blanco C. 1998. Hypothermia during or after severe perinatal anoxia prevents increase in cyclic GMP-related nitric oxide levels in the newborn rat striatum. Brain Res 791:303–307.

Loidl CF, Danilo Gavilanes AW, Van Dijk EH, Vreuls W, Blokland A, Johan SH, Steinbusch HWM, Blanco CE. 2000. Effects of hypothermia and gender on survival and behavior after perinatal anoxia in rats. Physiol Behav 68:263–269.

Moncada S, Higgs EA. 1991. Endogenours nitric oxide: physiology, pathology and clinical relevance. Eur J Clin Invest 21:361–374.

Moncada S, Palmer RMJ, Higgs EA. 1991. Nitric oxide: physiology, pathophysiology and pharmacology. Pharmacol Rev 43:109–142.

Moncada S, Higgs A, Furchgott R. 1997. XIV International union of pharmacology nomenclature in nitric oxide research. Am Soc Pharmacol Exp Ther 49:137–142.

Nandgaunkar BN, Rotschild T, Yu K, Higgins RDI. 1999. Indomethacin improves oxygen-induced retinopathy in the mouse. Pediatr Res 46:184–188.

Osborne N, Casson R, Wood J, Chidlow G, Graham M, Melena J. 2004. Retinal ischemia:mechanism of damage and potential therapeutic strategies. Ret Eye Res 23:91–147.

Palluy O, Rigaud M. 1996. Nitric oxide induces cultured cortical neuron apoptosis. Neurosci Lett 208:1–4.

Palmer C, Vannucci R. 1993. Potential new therapies for perinatal cerebral hypoxia-ischemia. Clin Perinatol 20:411–432.

Phelps DL, Watts JL. 1997.Early light reduction to prevent retinopathy of prematurity in very low birth weight infants. The Cochrane Library, Issue 1 Oxford.

Phelps DL, Lakatos L, Watts JL. 2000.D-penicillamine for preventing retinopathy in preterm infants. The Cochreane Library.

Pullen AH, Humphreys P. 1999. Protracted elevation of neuronal nitric oxide synthase immunoreactivity in axotomised motor neurons. J Anat 194:547–565.

Radomski MW, Vallance P, Whitley G, Foxwell N, Moncada S. 1993. Platelet adhesion to human vascular endothelium is modulated by constitutive and cytokine induced nitric oxide. Cardiovasc Res 27:1380–1382.

Raju TN, Langenberg P, Bhutani V, Quinn G. 1997. Vitamin E prophylaxis to reduce ROP: a reappraisal of published trials. J Pedriatr 131:844–850.

Rey-Funes M, Ibarra ME, Dorfman VB, López EM, López-Costa JJ, Coirini H, Loidl CF. 2010. Hypothermia prevents the development of ischemic proliferative retinopathy induced by severe perinatal asphyxia. Exp Eye Res 90:113–120.

Rivkin MJ. 1997. Hypoxic-ischemic brain injury in the term newborn. Neuropathology, clinical aspects, and neuroimaging. Clin Perinatol 24:607–625.

Rodrigo J, Alonso D, Fernandez AP, Serrano J, Richart A, Lopez JC, Santacana M, Martinez-Murillo R, Bentura ML, Ghiglione M, Uttenthal LO. 2001. Neuronal and inducible nitric oxide synthase expression and protein nitration in rat cerebellum after oxygen and glucose deprivation. Brain Res 909:20–45.

Rotschild T, Nandgaunkar BN, Yu K, Higgins RD. 1999. Dexamethasone reduces oxygen induced retinopathy in a mouse model. Pediatr Res 46:94–100.

Russell GA, Cooke RW. 1995. Randomised controlled trial of allopurinol prophylaxis in very preterm infants. Arch Dis Child Fetal Neonatal Ed 73:F27–F31.

Saito S, Kidd GJ, Trapp BD, Dawson TM, Bredt DS, Wilson DA, Traystman RJ, Snyder SH, Hanley DF. 1994. Rat spinal cord neurons contain nitric oxide synthase. Neuroscience 59:447–456.

Sennlaub F, Courtois Y, Goureau O. 2002. Inducible nitric oxide synthase mediates retinal apoptosis in ischemic proliferative retinopathy. J Neurosci 22:3987–3993.

Smith LE. 2003. Pathogenesis of retinopathy of prematurity. Semin Neonatol 8:469–473.

STOP ROP Multicenter Trial. 2000. Supplemental therapeutic oxygen for prethreshold retinopathy of prematurity (STOP-ROP), a randomized, controlled trial. I: primary outcomes. Pediatrics 105:295–310.

Uttenthal LO, Alonso D, Fernández AP, Campbell RO, Moro MA, Leza JC, Lozasoain I, Esteban FJ, Barroso JB, Valderrama R, Pedrosa JA, Peinado JA, Peinado MA, Serrano J, Rochardt A, Bentura ML, Santacana M, Martínez-Murillo R, Rodrigo J. 1998. Neuronal and inducible nitric oxide synthase and nitrotyrosine in the cerebral cortex of the aging rat. Microsc Res Techniq 43:75–88.

van den Tweel E, Nijboer C, Kavelaars A, Heijnen CJ, Groenendaal F, van Bel F. 2005a. Expression of nitric oxide synthase isoforms and nitrotyrosine formation after hypoxia-ischemia in the neonata rat brain. J Neuroimmunol 167:64–71.

Venturini CM, Knowles RG, Palmer RM, Moncada S. 1991. Synthesis of nitric oxide in the bovine retina. Biochem Biophys Res Commun 180:920–925.

Wakakura M. 2001. Experimental approaches to prophylactic neuroprotective treatment for retinal and optic nerve disorders. Nippon Ganka Gakkai Zasshi. 105:843–865.

WHO (World Health Organization). 1991. Consultation on birth asphyxia and thermal control of the newborn. Geneva, Switzerland: WHO.

Wilkinson-Berka JL, Alousis NS, Kelly DJ, Gilbert RE. 2003. COX-2 inhibition and retinal angiogenesis in a mouse model of retinopathy of prematurity. Invest Ophthalmol Vis Sci 44:974–979.

Yamamoto R, Bredt DS, Dawson TM, Snyder SH, Stone RA. 1993. Enhanced expression of nitric oxide synthase by rat retina following pterygopalatine parasympathetic denervation. Brain Res 631:83–88.

Younkin DP. 1992. Hypoxic-ischemic brain injury of the newborn-statement of the problem and overview. Brain Pathol 2:209–210.

Zhang X, Verge V, Wiesenfeld-Hallin Z, Ju G, Bredt D, Snyder SH, Hokfelt T. 1993. Nitric oxide synthase-like immunoreactivity in lumbar dorsal root ganglia and spinal cord of rat and monkey and effect of peripheral axotomy. J Comp Neurol 335:563–575.